Adiabatic cooling processes in frustrated magnetic systems with pyrochlore structure

E. Jurčišinová[1] and M. Jurčišin[1,2]

[1]*Institute of Experimental Physics, Slovak Academy of Sciences, Watsonova 47, 040 01 Košice, Slovakia*

[2]*Department of Theoretical Physics and Astrophysics, Faculty of Science, P.J. Šafárik University, Park Angelinum 9, 040 01 Košice, Slovakia*

(Received 24 May 2017; published 20 November 2017)

We investigate in detail the process of adiabatic cooling in the framework of the exactly solvable antiferromagnetic spin-$\frac{1}{2}$ Ising model in the presence of the external magnetic field on an approximate lattice with pyrochlore structure. The behavior of the entropy of the model is studied and exact values of the residual entropies of all ground states are found. The temperature variation of the system under adiabatic (de)magnetization is investigated and the central role of the macroscopically degenerated ground states in cooling processes is explicitly demonstrated. It is shown that the model parameter space of the studied geometrically frustrated system is divided into five disjunct regions with qualitatively different processes of the adiabatic cooling. The effectiveness of the adiabatic (de)magnetization cooling in the studied model is compared to the corresponding processes in paramagnetic salts. It is shown that the processes of the adiabatic cooling in the antiferromagnetic frustrated systems are much more effective especially in nonzero external magnetic fields. It means that the frustrated magnetic materials with pyrochlore structure can be considered as very promising refrigerants mainly in the situations with nonzero final values of the magnetic field.

DOI: 10.1103/PhysRevE.96.052128

I. INTRODUCTION

Magnetic systems with pyrochlore structure attract intense interest recently due to their intriguing low temperature properties such as the formation of macroscopically degenerated ground states, unusual entropy behavior, the existence of large magnetocaloric effect (MCE), anomaly behavior of the specific heat capacity, etc. [1–21]. These experimentally measured and theoretically described properties of the pyrochlore magnetic systems are usually related to the phenomenon of strong geometric frustration [22].

From a technological and an application point of view, maybe the most important thermodynamical property of such kind of magnetic materials is the MCE, i.e., cooling or heating of the material under variation of the external magnetic field, related to the changes of the magnetic entropy upon application of the magnetic field. The importance of the MCE is given especially by its great potential for using in magnetic refrigeration at low temperatures through the adiabatic (de)magnetization processes. Such kind of cooling seems to be very efficient energetically and that is why the intensive search for valid novel candidates for magnetic refrigeration is very important. Examples of such candidates are, e.g., $Dy_2Ti_2O_7$ [6,10,11,13,17], $Gd_2Ti_2O_7$ [5,14], $Nd_2Pb_2O_7$, $Gd_2Pb_2O_7$ [19], CePdAl [20], and $Er_2Ti_2O_7$ [21], which exhibit giant MCE.

Although the magnetic cooling in frustrated magnetic systems can be a very effective process, as we shall show, it is also a rather sophisticated process and for its effective realization one needs to have deep knowledge of thermodynamical properties of used material to be able to take use fully of its promising cooling potential. This is also the main reason why deep theoretical understanding of thermodynamical properties of various geometrically frustrated magnetic systems is really very needful. In this respect, it is always helpful if the theoretical background is based on an exactly solvable model in the framework of which the basic peculiarities of the frustrated systems can be understood on the exact fundamental level.

However, the set of even classical exactly solvable spin models on regular lattices is restricted to the one- and two-dimensional models [23–25] and, at the same time, there does not exist any relevant classical spin model on a regular two-dimensional lattice which would be exactly solved in the nonzero external magnetic field. On the other hand, the presence of the external magnetic field is crucial for the very existence of the MCE. Here, investigations of standard spin models on adequate approximate lattices, which, on one hand, take into account basic geometrical structure of the corresponding regular two- and three-dimensional lattices and, on the other hand, on which exact analysis of the models can be performed, are without doubt very helpful. Examples of such lattices are the so-called Husimi-type recursive lattices [26–28] on which the models can be always investigated by using the recursive relations technique (see, e.g., Refs. [29–31] and references cited therein). Moreover, in some special cases, models on recursive lattices are exactly solvable in fully analytic form [32–34]. Among such exactly solvable models belongs the antiferromagnetic spin-$\frac{1}{2}$ Ising model on the tetrahedron recursive lattice [34] (see Fig. 1), which represents an appropriate approximation of the three-dimensional lattice with pyrochlore structure shown explicitly in Fig. 2, and which takes into account its basic geometrical structure responsible for strong geometrical frustration. Note that some exact results on the tetrahedron recursive lattice were obtained early in the framework of the investigation of the spin ice problem [35,36]. It is also worth mentioning that the classical spin models very often represent very good approximation of real frustrated systems (see, e.g., Refs. [4,16,20]). Nevertheless, it is still necessary to bear in mind that the classical Ising and Ising-type models even on real lattices represent rather rough approximation of real magnetic materials, therefore, one can usually expect only qualitative accordance with real experiments.

In this paper, namely, the antiferromagnetic spin-$\frac{1}{2}$ Ising model in the presence of the external magnetic field on the tetrahedron recursive lattice will be used for an exact

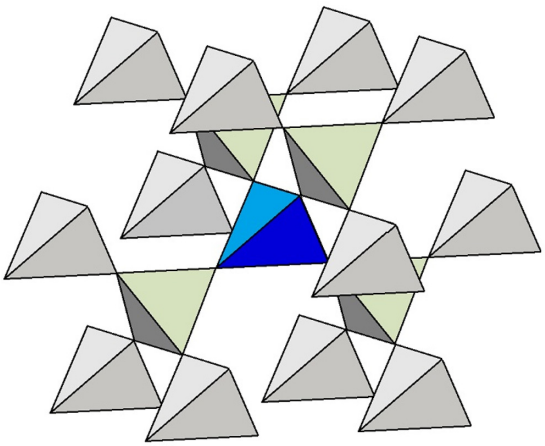

FIG. 1. The structure of the tetrahedron recursive lattice with coordination number $z = 6$.

theoretical investigation of the adiabatic (de)magnetization cooling processes and for an estimation of the efficiency of frustrated magnetic materials with pyrochlore structure for magnetic cooling at low temperatures in comparison to the paramagnetic salts which are standardly considered and used for magnetic refrigeration (see, e.g., Refs. [14,37–39] and references cited therein). As we shall see, the central role in the adiabatic (de)magnetization cooling processes is played by highly macroscopically degenerated ground states especially by the so-called single-point ground states, which are realized for exactly defined values of the external magnetic field and in the vicinity of which the adiabatic cooling is the most pronounced with potential possibility of obtaining ultralow temperatures.

The paper is organized as follows. In Sec. II, the model is briefly introduced. The properties of the entropy per site of the model are discussed and the residual entropies of all ground states of the model are found in Sec. III. Detailed analysis of adiabatic cooling processes in the framework of the studied model is performed in Sec. IV. Finally, obtained results are briefly reviewed and discussed in Sec. V.

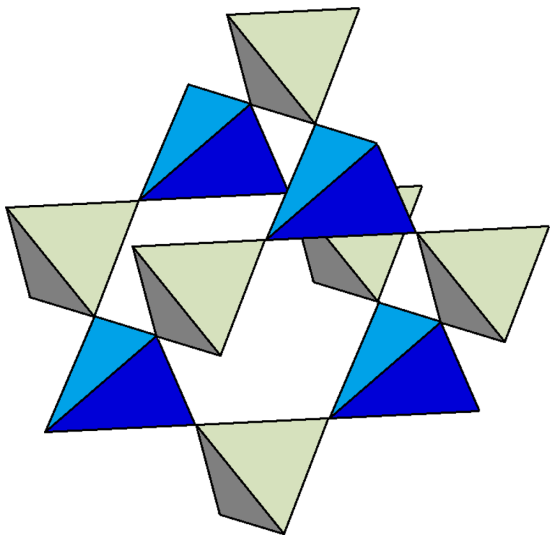

FIG. 2. The pyrochlore lattice structure.

II. DESCRIPTION OF THE MODEL

Thus, let us consider the classical antiferromagnetic spin-$\frac{1}{2}$ Ising model in the external magnetic field on the corner-sharing tetrahedron recursive lattice with coordination number $z = 6$ shown explicitly in Fig. 1 (see Ref. [34] for all details), which represents a suitable approximation of real three-dimensional pyrochlore structure demonstrated in Fig. 2, and which, as was already mentioned in the Introduction, properly takes into account its basic geometric structure responsible for strong geometric frustration.

The model is described by the following Hamiltonian:

$$\mathcal{H} = -J \sum_{\langle i\, j\rangle} s_i s_j - H \sum_i s_i, \tag{1}$$

where each variable s_i acquires one of two possible values ± 1, $J < 0$ is the nearest-neighbor antiferromagnetic interaction parameter, and H represents the external magnetic field. Standardly, in Eq. (1) the first sum runs over all nearest-neighbor spin pairs and the second sum runs over all spin sites.

The model can be analyzed numerically by using the recursion relations technique (see, e.g., Ref. [24]) but, as was shown and discussed in detail in Ref. [34], the exact analytic solution of the model exists. It was proven in Ref. [34] that the model exhibits exactly one unique solution for all values of the model parameters and the explicit form of the solution was found. In addition, a detailed analysis of the magnetization properties of the model was performed together with the analysis of the system of all ground states of the model. It was shown that the model exhibits the existence of the so-called single-point ground states, which are realized for some exact values of the external magnetic field, and which exist along with the well-known standard plateau ground states.

As we shall see in this paper, the existence of a degenerated system of single-point and plateau ground states in the frustrated antiferromagnetic materials with well-defined thermodynamical properties plays a crucial role in their adiabatic (de)magnetization processes and therefore for understanding of potential effectiveness of their use for magnetic cooling.

III. ENTROPY AND RESIDUAL ENTROPIES OF THE MODEL

The analysis of cooling processes in frustrated systems is based on the behavior of the entropy per site defined through the free energy per site of the studied model which in our case has the following explicit form:

$$\begin{aligned}\beta f = &-\ln(x^3 e^{3h} + 3x^2 e^{h-2K} + 3x e^{-h} + e^{6K-3h}) \\ &+ \tfrac{1}{2}\ln(x^4 e^{4h+6K} + 4x^3 e^{2h} + 6x^2 e^{-2K} \\ &+ 4x e^{-2h} + e^{6K-4h}),\end{aligned} \tag{2}$$

where $\beta = 1/(k_B T)$, T is the temperature, k_B is the Boltzmann constant, $K = \beta J$, $h = \beta H$, and x is the exact solution of the corresponding recursion relation (see Ref. [34] for all details),

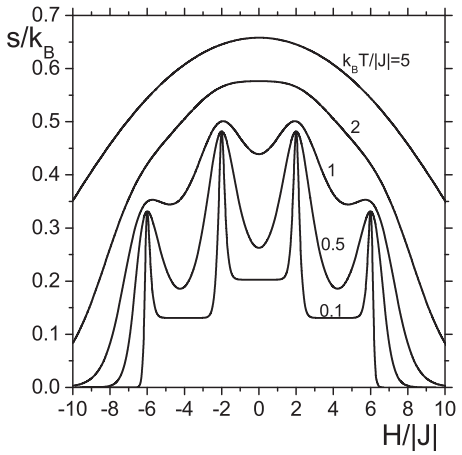

FIG. 3. Dependence of the entropy per site on the external magnetic field for various nonzero values of the reduced temperature.

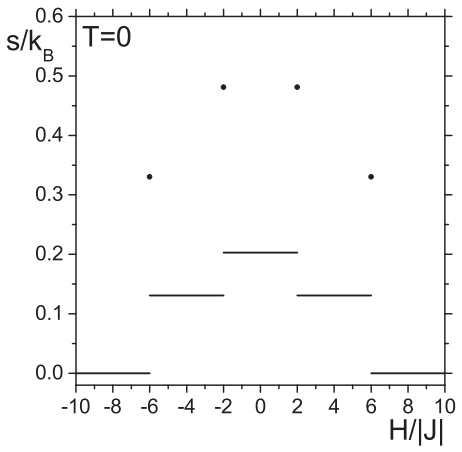

FIG. 4. The system of residual entropies of the model. The filled circles represent the residual entropies of the single-point ground states which are realized for $|H_{sp_1}/J| = 2$ and $|H_{sp_2}/J| = 6$, respectively.

the explicit form of which is given as

$$x = -\frac{b}{4a} + A + \frac{1}{2}\left(-4A^2 - B - \frac{C}{A}\right)^{1/2}, \tag{3}$$

where

$$A = \frac{1}{2\sqrt{3}}\left[-B + \frac{1}{a}\left(D + \frac{E}{D}\right)\right]^{1/2}, \tag{4}$$

$$B = \frac{8ac - 3b^2}{4a^2}, \tag{5}$$

$$C = \frac{b^3 - 4abc + 8a^2d}{8a^3}, \tag{6}$$

$$D = \left[\frac{F + (F^2 - 4E^3)^{1/2}}{2}\right]^{1/3}, \tag{7}$$

$$E = c^2 - 3bd + 12ae, \tag{8}$$

$$F = 2c^3 - 9bcd + 27b^2e + 27ad^2 - 72ace, \tag{9}$$

and

$$a = e^{2(3h+K)}, \quad b = e^{4h}[3 - e^{2(h+4K)}], \tag{10}$$

$$c = 3e^{2(h+K)}(1 - e^{2h}), \quad d = e^{8K} - 3e^{2h}, \tag{11}$$

$$e = -e^{2K}. \tag{12}$$

For completeness, let us note that the free energy per site (2) can be derived, e.g., by using the technique described in Ref. [40] (see also Ref. [41]).

The entropy per site is then standardly defined as follows:

$$s = -\frac{\partial f}{\partial T}, \tag{13}$$

and its dependence on the external magnetic field for various nonzero values of the reduced temperature is shown explicitly in Fig. 3. The entropy is a continuous function of the nonzero temperature as well as of the external magnetic field and, at the same time, one can immediately observe the formation of the system of nontrivial residual entropies for low enough values of the temperature for all ground states except of the saturated ground states with magnetization $m = \pm 1$ which are realized for $H/J > 6$ and $H/J < -6$, respectively (see Ref. [34]). It means that the model exhibits a highly macroscopically degenerated system of ground states with discrete values of the residual entropy per site shown explicitly in Fig. 4. Further, the model contains two plateau ground states with absolute values of magnetization $m = 0$ and $|m| = \frac{1}{2}$ (see Ref. [34] for details). The plateau ground state with $m = 0$ is realized for $|H/J| < 2$ and its exact residual entropy, which we denote as s_{pl_1} for convenience, is equal to

$$s_{pl_1} = \ln(3/2)/2\, k_B \approx 0.202733\, k_B. \tag{14}$$

It is worth mentioning that this exact theoretical result for the residual entropy is in perfect accordance with experimental measurements on the magnetic materials with pyrochlore structure, e.g., such as pyrochlore titanates $Dy_2Ti_2O_7$ [6,15,17]. Besides, this residual entropy is equal to the well-known Pauling entropy for the water ice, i.e., for the pyrochlore spin ice [42]. Thus, the studied model on the tetrahedron recursive lattice can be considered as very suitable for theoretical description of basic properties of pyrochlore magnetic systems. In this respect, let us note that this residual entropy on the real tetrahedron lattice was also estimated by Monte Carlo simulation [43] and the obtained result $0.20309 k_B$ is in very good agreement with exact Pauling entropy value (14).

On the other hand, the plateau ground states with $|m| = \frac{1}{2}$ which are realized for the values of the external magnetic field $2 < |H/J| < 6$ (see Ref. [34] for details) are less macroscopically degenerated in comparison to the zero magnetization plateau ground state and have the residual entropy per site equal to

$$s_{pl_2} = \ln(3\sqrt{3}/4)/2\, k_B \approx 0.130812\, k_B. \tag{15}$$

As was already mentioned, the model also exhibits the presence of two additional well-defined so-called single-point ground states, existence of which was proven in Ref. [34], which have unique thermodynamical properties and which are realized for exactly given absolute values of the external

magnetic field. (Note that the existence of the single-point ground states was exactly proven for the first time in Refs. [32,33] in the framework of the antiferromagnetic spin-$\frac{1}{2}$ Ising model on the kagomelike recursive lattice and later their existence was also proven in the antiferromagnetic models on geometrically frustrated one-dimensional systems [44,45].) These ground states play the role of the separating points between neighboring plateau ground states. As it follows from Figs. 3 and 4, they are highly macroscopically degenerated, i.e., with large values of the residual entropies in comparison to the plateau ground states, and, as we shall see in what follows, namely, this property of the single-point ground states is principal for proper understanding of the process of adiabatic cooling in magnetic frustrated systems. It is worth mentioning that the formation of the single-point ground states is very often visible in real experiments, e.g., in the behavior of the magnetization curves (see, e.g., Refs. [10,11]).

The first single-point ground state with exact magnetization

$$|m| = \frac{y^2 - 1}{y^2 + 1}, \tag{16}$$

where

$$y = -1 + 2\sqrt{2}\cos[(\pi - \arctan\sqrt{7})/3], \tag{17}$$

and with approximate value $|m| \approx 0.228438$ (see Ref. [34] for details), is realized for the absolute value of the external magnetic field $|H_{sp_1}/J| = 2$. Its exact residual entropy is equal to

$$s_{sp_1} = \frac{k_B}{2} \ln\left[\frac{y^2(y+3)^2}{4y+6}\right], \tag{18}$$

where y is given in Eq. (17) and its approximative numerical value is $s_{sp_1} \approx 0.481144 k_B$. Let us note that this single-point ground state is the most macroscopically degenerated ground state of the model, i.e., with the maximal value of the residual entropy, and represents the boundary (separating) ground state between the plateau ground states with magnetization $m = 0$ and $|m| = \frac{1}{2}$.

On the other hand, the second nontrivial single-point ground state with magnetization

$$|m| = \frac{8 + \sqrt{13}}{17} \approx 0.682679, \tag{19}$$

(again see Ref. [34] for details) emerges on the border between the plateau ground states with $|m| = \frac{1}{2}$ and saturated ground states with $|m| = 1$ for the absolute value of the external magnetic field $|H_{sp_2}/J| = 6$. Its residual entropy is equal to

$$s_{sp_2} = \frac{k_B}{2} \ln\left[\frac{19 + 13\sqrt{13}}{34}\right] \approx 0.330678 k_B. \tag{20}$$

The hierarchy of residual entropies of all ground states of the model is demonstrated in Fig. 4, where the filled circles represent the residual entropies of the single-point ground states.

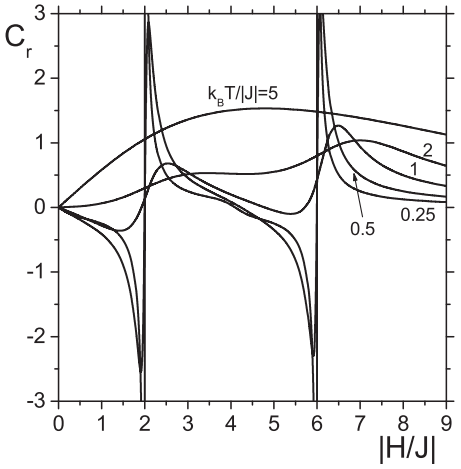

FIG. 5. The cooling rate C_r defined in Eq. (21) as the function of the absolute values of the external magnetic field for various temperatures.

IV. ANALYSIS OF ADIABATIC COOLING PROCESSES OF THE MODEL AND THEIR EFFICIENCY

The main aim of this paper is to perform detailed theoretical analysis of the adiabatic cooling processes, such as cooling through the adiabatic (de)magnetization, in the frustrated antiferromagnetic systems with pyrochlore structure in the framework of the studied exactly solvable model. The adiabatic magnetic cooling is standardly characterized by the cooling rate C_r defined as follows:

$$C_r \equiv \left(\frac{\partial T}{\partial H}\right)_S = -\frac{T}{c_H}\left(\frac{\partial s}{\partial H}\right)_T = -\frac{(\partial s/\partial H)_T}{(\partial s/\partial T)_H}, \tag{21}$$

where s is the entropy per site discussed in the previous section and c_H is the specific heat per site in a constant external magnetic field.

The dependence of the cooling rate (21) on the absolute value of the external magnetic field for various temperatures and on the reduced temperature for various absolute values of the external magnetic field are shown in Figs. 5 and 6,

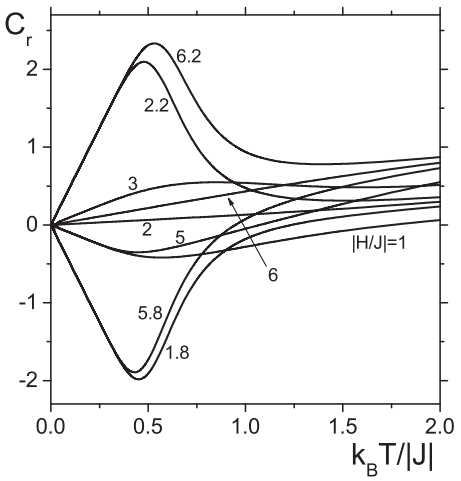

FIG. 6. The cooling rate as the function of the temperature for various absolute values of the external magnetic field.

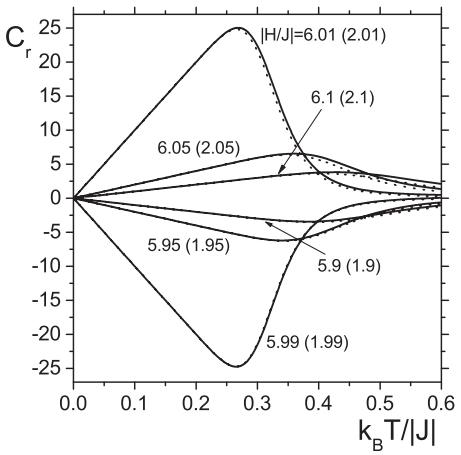

FIG. 7. The cooling rate as the function of the temperature for various absolute values of the external magnetic field in the vicinity of $|H_{sp_1}/J|$ and $|H_{sp_2}/J|$. Rapid increasing of the cooling rate as well as its universal behavior for the magnetic fields very close to $|H_{sp_1}/J|$ and $|H_{sp_2}/J|$ is demonstrated. The solid curves correspond to the external magnetic fields from the vicinity of $|H_{sp_2}/J| = 6$ and the dotted curves are related to the magnetic fields near $|H_{sp_1}/J| = 2$. The values of the external magnetic fields for dotted curves are placed into the parentheses.

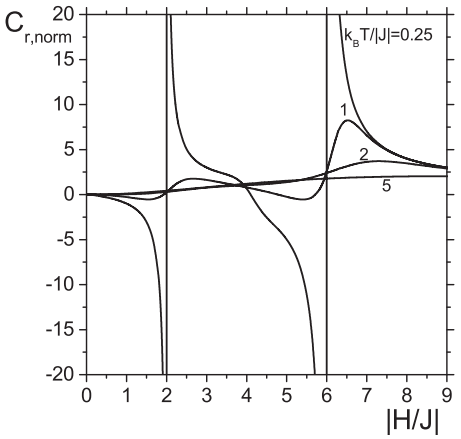

FIG. 8. The normalized cooling rate $C_{r,norm}$ as the function of the absolute value of the external magnetic field for various reduced temperatures.

respectively. Looking at these figures it is clear that, depending on the value of the external magnetic field, the cooling rate for small enough temperatures exhibits two different behaviors (see, e.g., the curves $k_BT/|J| = 0.25$, 0.5, and 1 in Fig. 5) related to the existence of highly macroscopically degenerated single-point ground states realized in the external magnetic field with the absolute values $|H_{sp_1}/J|$ and $|H_{sp_2}/J|$ discussed in the previous section. First, it is evident that when one decreases the intensity of the absolute value of the external magnetic field towards $|H_{sp_2}/J| = 6$ as well as towards $|H_{sp_1}/J| = 2$ the cooling rate increases rapidly, i.e., the system passes through strong cooling processes what is explicitly evident from Fig. 6 (see the curves for $|H/J| = 6.2$ and $|H/J| = 2.2$, respectively). Besides, the cooling effects become more intensive when the absolute values of the external magnetic field are very close to the $|H_{sp_1}/J|$ or $|H_{sp_2}/J|$ which are manifested themselves through the rapid increase of the cooling rate values (see curves $|H/J| = 2.01$ and 6.01 in Fig. 7). Moreover, as it follows from Fig. 7, the behavior of the cooling rate exhibits strong universality in the close vicinity of both $|H_{sp_1}/J|$ and $|H_{sp_2}/J|$. For low enough temperatures, the corresponding curves become almost indistinguishable.

Second, the opposite situation is observed for the absolute values of the external magnetic field from the left vicinity of $|H_{sp_1}/J|$ and $|H_{sp_2}/J|$. Here, the cooling rate obtains negative values as it follows from Figs. 5–7. It means that decreasing of the absolute values of the external magnetic field leads to the rapid heating of the system. In this case, the cooling effects are obtained by increasing of the absolute value of the external magnetic field towards $|H_{sp_1}/J|$ and $|H_{sp_2}/J|$.

Thus, in general, the most intensive cooling processes in the studied antiferromagnetic frustrated system are observed by the magnetic field changes towards the nearest single-point ground state magnetic field, i.e., towards $|H_{sp_1}/J|$ or $|H_{sp_2}/J|$.

Let us also compare the efficiency of the magnetic cooling in the present antiferromagnetic frustrated system with the effectiveness of the magnetic cooling in the paramagnetic salts, which are considered and used as standard refrigerant materials for the low temperature magnetic cooling. It is well known that the cooling rate of the ideal paramagnetic salt is simply given as follows: $C_{r,par} = T/H$. Therefore, the effectiveness of our frustrated system for the magnetic cooling in comparison to the ideal paramagnetic salt is given by the normalized cooling rate

$$C_{r,norm} \equiv C_r/C_{r,par}. \tag{22}$$

It is clear that in the region of the model parameters for which $C_{r,norm} > 1$, the magnetic cooling by the studied antiferromagnetic frustrated system is more effective than the magnetic cooling by the ideal paramagnetic salt.

In Figs. 8–10 the normalized cooling rate is demonstrated as the function of the absolute value of the external magnetic field for various temperatures and as the function of the reduced temperature for various absolute values of the external magnetic field. Everywhere where the absolute value of the normalized cooling rate is greater than one, the antiferromagnetic system with pyrochlore structure cools down faster than the ideal paramagnetic salt for the same model parameter values. As follows from Figs. 9 and 10, the normalized cooling rate increases rapidly when the external magnetic field approaches values $|H_{sp_1}/J| = 2$ or $|H_{sp_2}/J| = 6$ for low enough temperatures. Again, this behavior is directly related to the existence of two single-point ground states, the macroscopic degeneracies of which are sufficiently larger than macroscopic degeneracies of the plateau ground states which are separated by them.

It is also worth to mention that although the cooling rates near both single-point ground state values of the external magnetic field have a universal character (see Fig. 7) the effectiveness of the adiabatic cooling in comparison to the ideal paramagnetic salt is much larger in the vicinity of the single-point ground state with larger intensity of the external magnetic field, i.e., near $|H_{sp_2}/J| = 6$. The difference is explicitly shown in Fig. 10, where the solid curves correspond to the

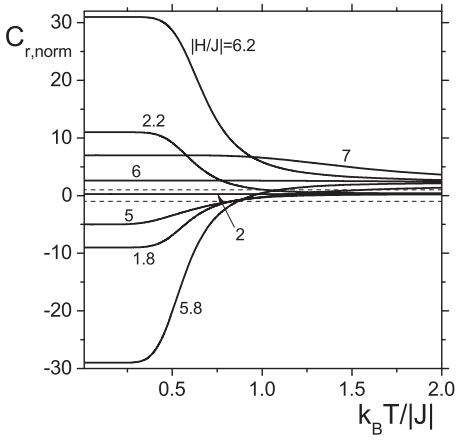

FIG. 9. The normalized cooling rate as the function of the temperature for various absolute values of the external magnetic field. The dashed lines correspond to $|C_{r,norm}| = 1$.

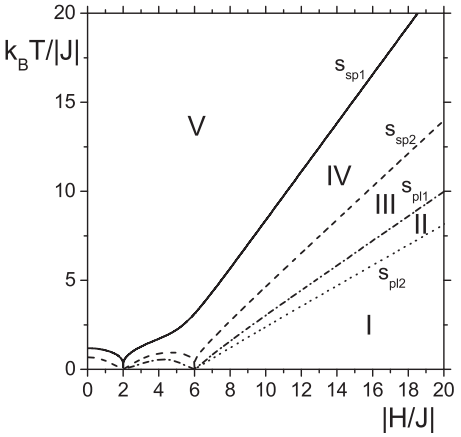

FIG. 11. The adiabatic curves for the residual entropy values which divide $|H/J| - k_B T/|J|$ plane into five disjunct regions in which the adiabatic curves have different properties (see the text).

external magnetic fields from the vicinity of $|H_{sp_2}/J| = 6$ and the dotted curves are related to the magnetic fields near $|H_{sp_1}/J| = 2$.

Now, let us discuss in detail the temperature variation under adiabatic (de)magnetization processes in the framework of the present model which is given by the adiabatic temperature change ΔT_{ad} defined as follows:

$$\Delta T_{ad} \equiv \int_{H_i}^{H_f} \mathrm{C_r}\, dH, \tag{23}$$

where $\mathrm{C_r}$ is the cooling rate defined in Eq. (21) and H_i and H_f are initial and final values of the external magnetic field, respectively, during the studied adiabatic process. At the same time, the character of the adiabatic cooling processes strongly depends on the initial values of the external magnetic field as well as on the initial values of the temperature. Here, the key role is played by the residual entropies of all ground states of the model which divide the $|H/J|$ versus $k_B T/|J|$ plane into five specific disjunct regions (see Fig. 11) and in which the adiabatic curves have different behavior with different final cooling result, i.e., with different reached final temperature.

In the region of the model parameters denoted as I in Fig. 11 (the region below dotted curve), the entropies of the corresponding states are always less than the residual entropy of the plateau ground state with absolute value of magnetization $|m| = \frac{1}{2}$, i.e., $s/k_B < s_{pl_2}/k_B \approx 0.130812$. Note that such states exist only for $|H/J| > 6$. All adiabatic curves from this region end arbitrarily close to zero temperature when the external magnetic field decreases to $|H_{sp_2}/J| = 6$. Thus, starting in this region of model parameters the system can be cooled down to the final state with arbitrarily low nonzero temperature and with the absolute value of the external magnetic field close but always larger than $|H_{sp_2}/J| = 6$. This behavior is shown in Fig. 12 (see the adiabatic curves with $s/k_B = 0.065$ and 0.13), where various adiabatic curves of the model are shown (solid lines with explicit values of the entropy) together with the residual entropy adiabatic curves denoted as red dotted lines which correspond to the adiabatic curves shown in Fig. 11.

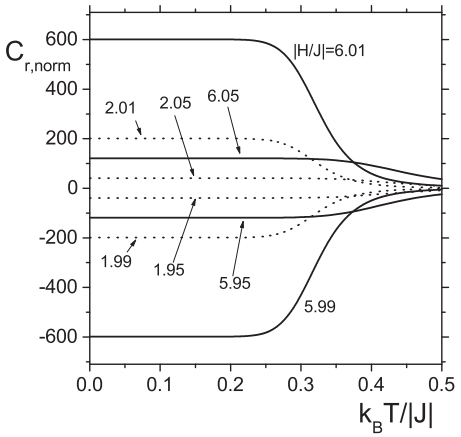

FIG. 10. The normalized cooling rate as the function of the temperature for the absolute values of the external magnetic field close to $|H_{sp_1}/J|$ and $|H_{sp_2}/J|$, respectively. The solid curves correspond to the external magnetic fields from the vicinity of $|H_{sp_2}/J| = 6$ and the dotted curves are related to the magnetic fields near $|H_{sp_1}/J| = 2$.

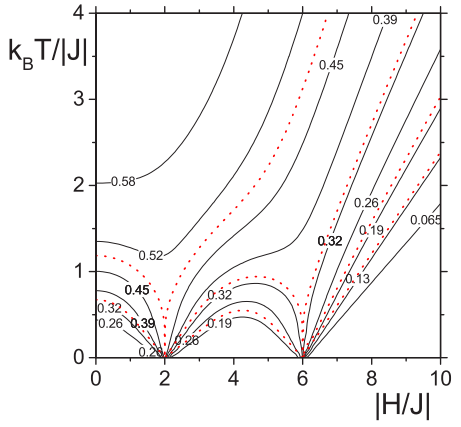

FIG. 12. Adiabatic curves for various values of the entropy per site s/k_B (solid lines). The dotted curves represent the adiabatic curves with the corresponding residual entropy values (see Fig. 11).

The states from the second region of model parameters, denoted as II in Fig. 11, have values of entropy between the residual entropies of two plateau ground states of the model, i.e., between s_{pl_1} and s_{pl_2}, and such kind of states are present in the model for $2 < |H/J| < 6$ (only below the dashed-dotted curve in Fig. 11) as well as for $|H/J| > 6$. In this case, it is evident that the process of adiabatic cooling depends on the initial value of the external magnetic field H_i. If $|H_i/J| > 6$, then decreasing of the temperature is obtained by decreasing of the absolute value of the external magnetic field to $|H_{sp_2}/J| = 6$ in an analogous way as in the previous case. However, the adiabatic cooling process is different when $2 < |H_i/J| < 6$. Here, the cooling down to very low temperatures can be realized by increasing of the absolute value of the magnetic field towards $|H_{sp_2}/J| = 6$ or by decreasing of the absolute value of the magnetic field towards $|H_{sp_1}/J| = 2$ (see the adiabatic curve with $s/k_B = 0.19$ in Fig. 12).

The third region denoted as III in Fig. 11 represents the region of the model parameters for which the states of the system have entropy values between s_{pl_1} and s_{sp_2} (in Fig. 11 it is given by the region between the dashed curve and dashed-dotted curve for $|H/J| > 2$ and by the region below the dashed curve for $|H/J| < 2$). One can immediately see that it is the first region of parameters for which such states exist for arbitrary values of the magnetic field for nonzero temperatures. Here, again the adiabatic cooling process to very low temperatures strongly depends on the initial absolute value of the magnetic field, namely, it can be realized by changing of the value of the magnetic field towards the nearest single point value of the external magnetic field, i.e., towards $H_{sp_1}/J = \pm 2$ or $H_{sp_2}/J = \pm 6$ (see the adiabatic curves with $s/k_B = 0.26$ and 0.32 in Fig. 12).

The region of model parameters for which the values of the entropy are between the residual entropies s_{sp_1} and s_{sp_2} is denoted as IV in Fig. 11. Here, it is evident that the cooling down to very low temperatures is surely possible only when the absolute values of the magnetic field tend to $|H_{sp_1}/J| = 2$ (by decreasing or increasing of the absolute value of the external magnetic field towards $|H_{sp_1}/J| = 2$). On the other hand, the very low temperatures can be also obtained when $|H/J|$ tends to $|H_{sp_2}/J| = 6$ but only when the initial state has the entropy value very close to the residual entropy s_{sp_2}. Typical adiabatic curves from this region are shown in Fig. 12 (see the adiabatic curves with $s/k_B = 0.39$ and 0.45).

Finally, there exists the region of the model parameters in which the entropy of the system is always larger than the residual entropy of the most macroscopically degenerated ground state of the model, i.e., larger than s_{sp_1}. This region, denoted as V, is placed over the solid curve in Fig. 11. Here, the adiabatic cooling down to very low temperatures is possible only when the initial state has the entropy value very close to the residual entropy s_{sp_1} and the corresponding cooling process is realized near the single-point absolute value of the magnetic field $|H_{sp_1}/J| = 2$. Each adiabatic curve from this region obtains a minimal value of the adiabatic temperature for some value of the external magnetic field which represents the minimal value of the temperature which can be reached by given cooling process. Again, typical adiabatic curves from this region can be seen in Fig. 12 (see the adiabatic curves with $s/k_B = 0.52$ and 0.58, respectively).

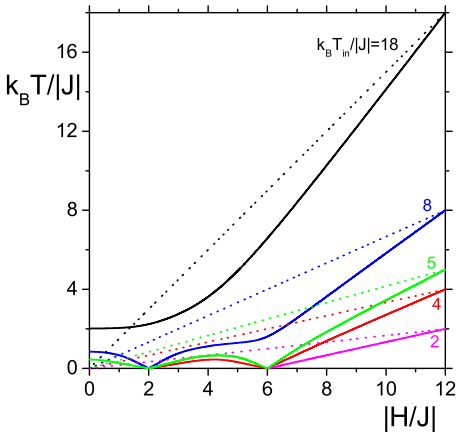

FIG. 13. Comparison of adiabatic curves from different regions I–V (see Fig. 11) with the corresponding adiabatic curves of the ideal paramagnetic salt (dotted lines). The initial absolute value of the magnetic field is fixed and equal to $|H_i/J| = 12$.

As it follows from the above discussion, the adiabatic cooling in the framework of frustrated antiferromagnetic systems is a rather complicated but very sophisticated process which strictly depends on the initial conditions before cooling. It means that to be able to use effectively such materials for cooling to very low temperatures it is necessary first to know their basic thermodynamical properties, such as the system of all ground states with their residual entropies which, as was shown above, play the key role in the adiabatic cooling processes. Then, the most effective strategy of cooling can be chosen depending on the initial conditions of the system or, contrariwise, the suitable initial conditions can be adjusted for the experimentally realizable effective process of adiabatic cooling. It is worth mentioning that the processes of the adiabatic cooling are the most effective for such initial states of the system which have values of the entropy very close to the corresponding residual entropy of some model ground state.

Let us also note that, from a pure theoretical point of view, the absolute zero temperature can be in principle reached only when the entropy of an initial state is exactly equal to one of the residual entropies of the ground states of the model and the corresponding cooling process is realized towards the nearest possible single-point value of the external magnetic field, i.e., towards $|H_{sp_1}/J| = 2$ or $|H_{sp_2}/J| = 6$.

It is also instructive to compare the efficiency of the adiabatic cooling in the framework of the present frustrated antiferromagnetic system with the corresponding cooling processes in standardly used paramagnetic salts. In this respect, in Fig. 13 the corresponding comparison is performed for fixed initial absolute value of the external magnetic field ($|H_i/J| = 12$) and for various initial values of the reduced temperature chosen such that the initial conditions belong into different regions I−V discussed above (see Fig. 11). In Fig. 13, the solid lines correspond to the adiabatic temperature of the studied pyrochlore system and the corresponding adiabatic temperature curves for the ideal paramagnetic salt with the same initial conditions are demonstrated by dotted lines. It is evident from this figure that the adiabatic cooling of the paramagnetic salts is more effective only for relatively

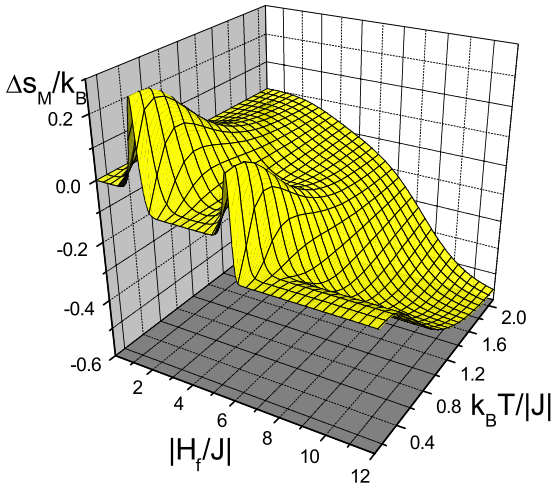

FIG. 14. The isothermal magnetic change Δs_M defined in Eq. (24) for $H_i = 0$ as the function of the reduced temperature and of the absolute value of the final magnetic field $|H_f/J|$.

small absolute values of the external magnetic field. This fact is obvious because the paramagnetic salts have unique macroscopically degenerated single-point ground state with residual entropy per site equal to $k_B \ln 2$ which is realized directly in zero external magnetic field, i.e., the process of the adiabatic cooling (as well as the MCE) is the most pronounced in the vicinity of the zero external magnetic field. On the other hand, as for the studied antiferromagnetic system with pyrochlore structure, the processes of the adiabatic cooling are significantly more effective in comparison to the analogous processes in paramagnetic salts for higher absolute values of the external magnetic field and the effectiveness is largest for magnetic fields in the vicinity of the single-point ground state magnetic field values $|H_{sp_1}/J| = 2$ and $|H_{sp_2}/J| = 6$. Note that this conclusion is valid regardless of the region from which the initial conditions are chosen.

Finally, let us also briefly discuss another important quantitative characteristic of the MCE, namely, the isothermal magnetic entropy change Δs_M defined as follows:

$$\Delta s_M(T,\Delta H) = \int_{H_i}^{H_f} \left(\frac{\partial s}{\partial H}\right)_T dH, \qquad (24)$$

where H_i and H_f are again initial and final values of the external magnetic field, respectively. Its simultaneous dependence on the absolute value of the final external magnetic field $|H_f/J|$ and on the temperature is shown in Fig. 14 for $H_i = 0$, i.e., $\Delta H = H_f$. At the same time, in Figs. 15 and 16, the dependence of Δs_M on the $|H_f/J|$ for various values of the temperature and on the temperature for various values of $|\Delta H/J|$ is shown. All these figures also demonstrate the central role of the highly macroscopically degenerated single-point ground states of the model for the existence of giant MCE which manifest themselves in magnetic field induced large changes in the magnetic entropy in the vicinity of the single-point ground state absolute values of the magnetic field.

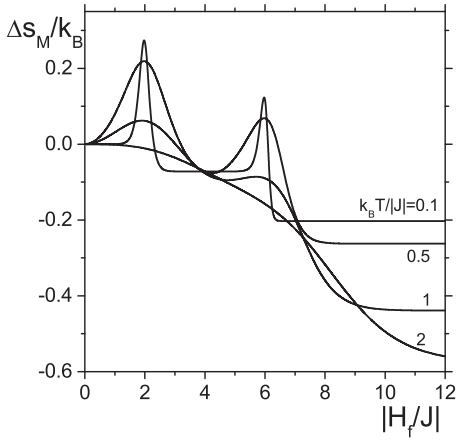

FIG. 15. The isothermal magnetic change Δs_M for $H_i = 0$ as the function of the absolute value of the final magnetic field $|H_f/J|$ for various values of the reduced temperature.

V. CONCLUSION

In this paper, we have investigated in detail adiabatic (de)magnetization cooling processes in the geometrically frustrated antiferromagnetic spin-$\frac{1}{2}$ Ising model with the presence of the external magnetic field on the tetrahedron recursive lattice which represents a suitable approximation of real systems with pyrochlore structure and which takes into account its basic geometrical structure responsible for strong frustration.

First of all, using the exact expression for the free energy per site of the model, the behavior of the entropy is investigated and the exact expressions for the residual entropies of all ground states of the model are found (see Figs. 3 and 4). It is shown that the model exhibits the presence of two unique highly macroscopically degenerated single-point ground states with well-defined thermodynamical properties along with the existence of two plateau ground states which also have nonzero residual entropies.

The cooling rate, i.e., the adiabatic change of the temperature as a response on the variation of the magnetic field,

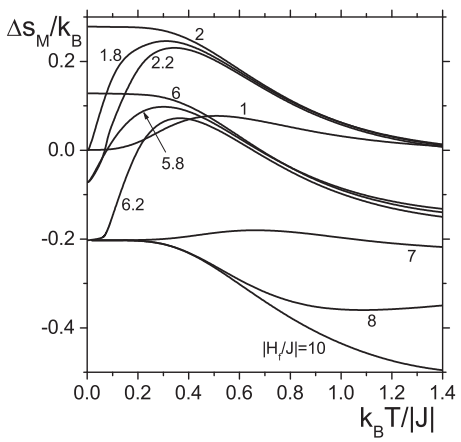

FIG. 16. The isothermal magnetic change Δs_M for $H_i = 0$ as the function of the reduced temperature for various absolute values of the final magnetic field $|H_f/J|$.

is studied as the function of the temperature and of the external magnetic field and it is shown that the adiabatic magnetic cooling is most pronounced in the vicinity of the single-point ground state values of the magnetic fields: $|H_{sp_1}/J| = 2$ and $|H_{sp_2}/J| = 6$. This is manifested explicitly by the rapid changes of the cooling rate near these special values of the external magnetic field (see Figs. 5–7). At the same time, it is also shown that the cooling processes exhibit almost universal behavior in the near vicinity of both single-point ground state values of the external magnetic field (see Fig. 7). The efficiency of the cooling processes in the studied antiferromagnetic frustrated system is compared to the corresponding processes in the ideal paramagnetic salt. It is shown that the geometrically frustrated antiferromagnetic system with the pyrochlore structure cools down much more faster than the ideal paramagnetic salts especially near the nonzero single-point ground state values of the external magnetic field (see Figs. 8–10).

The sensitivity of the adiabatic temperature to field variations in the processes of the adiabatic (de)magnetization cooling is investigated and it is shown that the model parameter space is divided into five disjunct regions with specific behavior of the adiabatic curves (see Figs. 11–13) which are defined by the adiabatic curves corresponding to the nontrivial residual entropies of all ground states of the model. It means that the results (reached low temperatures) and effectiveness of the adiabatic cooling processes in frustrated antiferromagnetic systems strongly depend on the chosen initial conditions as well as on the cooling strategy. Thus, the adiabatic cooling in this case represents a sophisticated process, unlike the straightforward cooling process in paramagnetic salts. Therefore, it is necessary first to know basic thermodynamical characteristics of the system (especially the system of all ground states of the model, the positions of all single-point ground states of the model, as well as their residual entropies) to be able to use effectively such materials with great potential for adiabatic cooling to ultralow temperatures.

Finally, let us also note that our theoretical results obtained in the framework of the classical antiferromagnetic model on the recursive lattice with pyrochlore structure are in very good qualitative agreement with recent experimental results obtained on the pyrochlore material $Er_2Ti_2O_7$ (see, e.g., Figs. 2 and 3 in Ref. [21]). It means that even classical spin systems represent a suitable platform for investigation of fundamental physical properties of real frustrated magnetic materials. However, on the other hand, it is also necessary to bear in mind that there exist materials which, despite the fact that they have the same pyrochlore structure, under the influence of the magnetic field in some special direction exhibit thermodynamical properties of magnetic systems with two-dimensional kagomelike structure (see, e.g., Refs. [10,11]), i.e., for description of their properties the kagome lattice represents much more appropriate basis [46,47].

ACKNOWLEDGMENTS

The authors gratefully acknowledge the hospitality of the Bogoliubov Laboratory of Theoretical Physics of the Joint Institute for Nuclear Research, Dubna, Russian Federation. M.J. also gratefully acknowledges the hospitality of the TH division in CERN. The work was supported by the VEGA Grant No. 2/0065/17 of Slovak Academy of Sciences and by the realization of the Project ITMS No. 26220120029, based on the supporting operational Research and development program financed from the European Regional Development Fund.

[1] N. P. Raju, E. Gmelin, and R. K. Kremer, Phys. Rev. B **46**, 5405 (1992).
[2] A. P. Ramirez, Annu. Rev. Mater. Sci. **24**, 453 (1994).
[3] M. J. Harris, S. T. Bramwell, P. C. W. Holdsworth, and J. D. M. Champion, Phys. Rev. Lett. **81**, 4496 (1998).
[4] R. Siddharthan, B. S. Shastry, A. P. Ramirez, A. Hayashi, R. J. Cava, and S. Rosenkranz, Phys. Rev. Lett. **83**, 1854 (1999).
[5] N. P. Raju, M. Dion, M. J. P. Gingras, T. E. Mason, and J. E. Greedan, Phys. Rev. B. **59**, 14489 (1999).
[6] A. P. Ramirez, A. Hayashi, R. J. Cava, R. Siddharthan, and B. S. Shastry, Nature (London) **399**, 333 (1999).
[7] B. C. den Hertog and M. J. P. Gingras, Phys. Rev. Lett. **84**, 3430 (2000).
[8] R. G. Melko, B. C. den Hertog, and M. J. P. Gingras, Phys. Rev. Lett. **87**, 067203 (2001).
[9] J. E. Greedan, J. Mater. Chem. **11**, 37 (2001)
[10] K. Matsuhira, Z. Hiroi, T. Tayama, S. Takagi, and T. Sakakibara, J. Phys.: Condens. Matter **14**, L559 (2002).
[11] Z. Hiroi, K. Matsuhira, S. Takagi, T. Tayama, and T. Sakakibara, J. Phys. Soc. Jpn. **72**, 411 (2003).
[12] R. Higashinaka, H. Fukazawa, and Y. Maeno, Phys. Rev. B **68**, 014415 (2003).
[13] T. Sakakibara, T. Tayama, Z. Hiroi, K. Matsuhira, and S. Takagi, Phys. Rev. Lett. **90**, 207205 (2003).
[14] S. S. Sosin, L. A. Prozorova, A. I. Smirnov, A. I. Golov, I. B. Berkutov, O. A. Petrenko, G. Balakrishnan, and M. E. Zhitomirsky, Phys. Rev. B **71**, 094413 (2005).
[15] X. Ke, R. S. Freitas, B. G. Ueland, G. C. Lau, M. L. Dahlberg, R. J. Cava, R. Moessner, and P. Schiffer, Phys. Rev. Lett. **99**, 137203 (2007).
[16] X. Ke, M. L. Dahlberg, E. Morosan, J. A. Fleitman, R. J. Cava, and P. Schiffer, Phys. Rev. B **78**, 104411 (2008).
[17] X. Ke, D. V. West, R. J. Cava, and P. Schiffer, Phys. Rev. B **80**, 144426 (2009).
[18] J. S. Gardner, M. J. P. Gindras, and J. E. Greedan, Rev. Mod. Phys. **82**, 53 (2010).
[19] A. M. Hallas, A. M. Arevalo-Lopez, A. Z. Sharma, T. Munsie, J. P. Attfield, C. R. Wiebe, and G. M. Luke, Phys. Rev. B **91**, 104417 (2015).
[20] S. Lucas, K. Grube, C.-H. Huang, A. Sakai, W. Wunderlich, E. L. Green, J. Wosnitza, V. Fritsch, P. Gegenwart, O. Stockert, and H. v. Löhneysen, Phys. Rev. Lett. **118**, 107204 (2017).
[21] B. Wolf, U. Tutsch, S. Dörschung, C. Krellner, F. Ritter, W. Assmus, and M. Lang, J. Appl. Phys. **120**, 142112 (2016).
[22] G. Toulouse, Commun. Phys. **2**, 115 (1977).

[23] B. M. McCoy and T. T. Wu, *The Two-Dimensional Ising Model* (Harvard University Press, Cambridge, Massachusetts, 1973).
[24] R. J. Baxter, *Exactly Solved Models in Statistical Mechanics* (Academic, London, 1982).
[25] *Frustrated Spin Systems*, edited by H. T. Diep (World Scientific, Singapore, 2004).
[26] K. Husimi, J. Chem. Phys. **18**, 682 (1950).
[27] F. Harary and G. E. Uhlenbeck, Proc. Natl. Acad. Sci. USA **39**, 315 (1953).
[28] J. W. Essam and M. E. Fisher, Rev. Mod. Phys. **42**, 272 (1970).
[29] J. L. Monroe, Phys. A (Amsterdam) **256**, 217 (1998).
[30] M. Pretti, J. Stat. Phys. **111**, 993 (2003).
[31] N. S. Ananikian, V. V. Hovhannisyan, and H. A. Lazaryan, Int. J. Mod. Phys. B **24**, 5913 (2010).
[32] E. Jurčišinová, M. Jurčišin, and A. Bobák, Phys. Lett. A **377**, 2712 (2013).
[33] E. Jurčišinová, M. Jurčišin, and A. Bobák, J. Stat. Phys. **154**, 1096 (2014).
[34] E. Jurčišinová and M. Jurčišin, Phys. Rev. E **89**, 032123 (2014).
[35] L. D. C. Jaubert, J. T. Chalker, P. C. W. Holdsworth, and R. Moessner, Phys. Rev. Lett. **100**, 067207 (2008).
[36] L. D. C. Jaubert, M. J. Harris, T. Fennell, R. G. Melko, S. T. Bramwell, and P. C. W. Holdsworth, Phys. Rev. X **3**, 011014 (2013).
[37] K. A. Gschneider, Jr. and V. K. Pecharsky, J. Appl. Phys. **85**, 5365 (1999)
[38] M. E. Zhitomirsky, Phys. Rev. B **67**, 104421 (2003).
[39] Y.-C. Chen, J. Prokleška, W.-J. Xu, J.-L. Liu, J. Liu, W.-X. Zhang, J.-H. Jia, V. Sechovský, and M.-L. Tong, J. Mater. Chem. C **3**, 12206 (2015).
[40] N. S. Ananikian, N. Sh. Izmailian, and K. A. Oganessyan, Phys. A (Amsterdam) **254**, 207 (1998).
[41] P. D. Gujrati, Phys. Rev. Lett. **74**, 809 (1995).
[42] L. Pauling, *The Nature of the Chemical Bound* (Cornell University Press, Ithaca, NY, 1960), pp. 301–304.
[43] R. Liebmann, *Statistical Mechanics of Periodic Frustrated Ising Systems* (Springer, Berlin, 1986), pp. 119–120.
[44] E. Jurčišinová and M. Jurčišin, Phys. Rev. E **90**, 032108 (2014).
[45] E. Jurčišinová and M. Jurčišin, J. Stat. Mech. (2016) 013101.
[46] M. Udagawa, M. Ogata, and Z. Hiroi, J. Phys. Soc. Jpn. **71**, 2365 (2002).
[47] E. Jurčišinová and M. Jurčišin, Phys. A (Amsterdam) **486**, 296 (2017).